J. Integr. Sci. Technol. 2023, 11(3), 514 Article

Journal of Integrated
SCIENCE & TECHNOLOGY

Design and simulation of Multi-Input Converter for Renewable energy sources

Chirag Gupta,* Vikas Kumar Aharwal

Department of Electrical Engineering, Dr. A. P. J. Abdul Kalam University, Indore, Madhya Pradesh, India.

Received on: 09-October-2022, Accepted and Published on: 03-Apr-2023

ABSTRACT

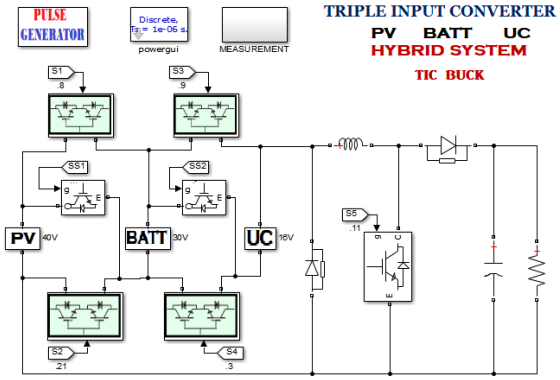

The energy inputs from variety of renewable resources (hybrid systems) requires efficient power converter interface towards integrated management of power load. This study reports a novel power conditioner topology that integrates a variety of renewable energy sources. This allows for higher reliability than what could be attained by a single power source while maximizing the utilization of each source's operational capabilities. It is shown a novel three-input DC/DC converter for hybrid PV/Battery/UC applications. Six power switches are used in the designed converter. Additionally, switching modulation is in no way constrained. By adjusting the duty ratios of the switches, it is possible to manage the battery power, set the UC power, calibrate the output voltage, and monitor the maximum power of the PV source. The input power sources have the ability to supply the load either simultaneously or sequentially while simultaneously charging or discharging the battery.

Keywords: DC-DC Converter, Hybrid energy sources, Multi-input converter (MIC), MATLAB.

INTRODUCTION

With the world's population growing so quickly, global energy consumption is rising substantially. For meeting future energy demands, renewable energy sources are now in the lead. Hybrid energy systems (HES) received significantly more attention in DC distributed generation due to their capacity to offer loads[1] through to receive dependable power.[2] Energy from a variety of voltage sources with different voltage-current (V-I) characteristics, such as fuel cells, solar, wind, and battery storage systems coupled in various combinations, will be supplied to the load through the power electronic converter interface in the HES. The power system's dependability is increased by the HES's capacity to carry power both ways.

In order to simplify and reduce the cost of hybrid power systems, the use of multiple input converters (MICs) to replace numerous single input converters has recently attracted a growing amount of interest. Compared to typical methods that make use of numerous individual converters, MICs have the following advantages: (i) MICs have a simpler design, a lower price, and a higher power density since active switches and reactive components are multiplexed or shared.[3–5] (ii) Due to its centralized control and unified power management, MICs can enhance dynamic performance and prevent complicated communication among several sources. Because it is economical and has developed prospects, MIC is a good replacement for small-scale renewable energy systems.[6–10]

Numerous MIC topologies, both isolated and non-isolated, have been proposed. Magnetically linked circuits (MCC) serve as the foundation for isolated topologies, whereas electrically connected circuits serve as the foundation for non-isolated topologies (ECC). In MCC, time domain multiplexing and flux addition are frequently utilized to convert energy from sources to loads. The transformer and additional peripheral circuitry included making the MCC complicated, heavy, expensive, and more dependent on circuit conditions. Due to its modular design, ECC is less expensive and more appealing than MCC because it does not require a transformer.[11,12]

It should be noted that obtaining a regulated dc output is key in the use of such dc-dc converter for combining different generation sources in order to cater to the energy requirements of the load. The significant variance in input voltage, however, makes it impossible to obtain the regulated dc output in the case that one of the energy sources diminishes. Consequently, the solution is to

*Corresponding Author: Chirag Gupta, Indore
Email: cgupta.011@gmail.com

Cite as: *J. Integr. Sci. Technol., 2023, 11(3), 514.*

 ISSN: 2321-4635
http://pubs.thesciencein.org/jist

integrate the sources by paralleling them using a transformer which is the basis of isolated TIC.[13] The number of input-stage circuits for an isolated TIC is related to the number of independent generation sources we want to operate in parallel. Each independent DC source, coupled by means of a full-bridge dc / ac converter, can act as a DC current source which enables the isolated TIC to have different generation sources with different voltage levels.[14,15] This is especially relevant when one of the energy sources is solar photovoltaic. The output voltage of a solar module depends on solar insolation and ambient temperature. Hence, there is constant variation in input voltage for solar photovoltaic sources. Consequently, it is imperative to use a high-ratio DC-DC converter to achieve stable dc-voltage.[16] Also, it is important that the input-stage windings of the transformer are wound on the same magnetic core with the output-stage winding so that there is no flux leakage and the input flux can fully pass through to the output flux. Such an isolated TIC has many advantages over non-isolated TIC: a) the voltage levels of various sources may differ. b) the converter can synchronize with different sources individually and simultaneously c) access to soft-switching d) galvanic or electrical isolation is a natural consequence. It should be noted that it suffers from stress due to high voltage, switching losses, electromagnetic interference issues, and lower conversion efficiency. These are not present in non-isolated TIC.[17]

SPV alone might not be enough for any load, because the variations in temperature and irradiance have an impact on their power-generating capacity. Therefore, energy storage devices (ESD) are necessary to continuously satisfy load demand. If the battery is connected directly to the dc bus, the battery's charging and draining cannot be managed. Authors[18,19] in recommended using a lithium-ion battery system for a BDDC. In the shown configuration, two separate DC-DC converters represent the SPV system and the ESD. To integrate PV and energy storage systems with the grid, the average efficiency of all non-isolated topologies and various multiport converters were investigated.

The majority of TIC/DIC topologies given in prior research work have drawbacks related to the choice of voltage levels, operating mode restrictions, complexity of switching schemes, poor switch selection, insufficiency of analysis, and component numbers.[20]

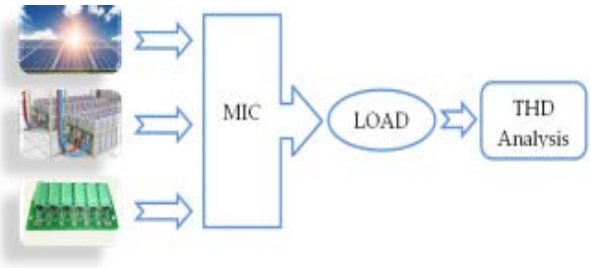

Figure 1. Block diagram of suggested TIC topology

This paper examines and presents the topologies of multi-input DC-DC converters used in applications involving renewable energy systems, along with some recent advances in the field.

CONVERTER TOPOLOGY

TIC Configuration

The suggested TIC architecture is shown in Figure 2 in this section. Three sources, each with a different voltage-current characteristic, are used to feed the load, either sequentially or concurrently. The three input sources employed in TIC are solar photovoltaic (PV) systems, battery storage systems, and ultra-capacitor banks. a single inductor (L), two diodes, two unidirectional switches (SS1 and SS2), four bidirectional switches (S1 to S4), a huge dc link capacitor (C), and a load resistor make up the converter component.

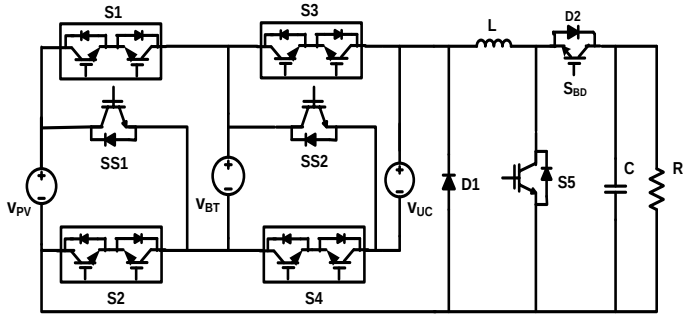

Figure 2. Topological configuration of designed triple input converter (TIC)

The bidirectional switches can be realized by connecting the two unidirectional conducting and bidirectional blocking switches in the antiparallel. Switches SS1 and SS2 are crucial for the sources' series operation, whereas switches S1 to S4 are activated for the sources' parallel operation.

Control Strategy

In the designed TIC, an independent switching scheme is employed for appropriate control of switches which is regarded as important from the utilization point of view. This also helps in regulating the power at the load terminals. Appropriate time sharing of switch driving pulses for the converter ensures the proper sequencing of converter operating states in different modes.

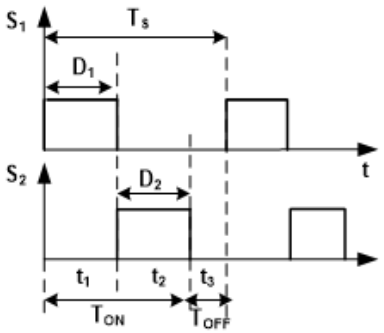

Figure 3. Independent switching scheme

The duration of time for different working states can be demarcated through duty cycle. For independent synchronization switching shown in Figure 3 duty cycles can be defined as;

$$t_1 = (D_1)T_s$$
$$t_2 = (D_2)T_s \quad \ldots(5.13)$$
$$t_3 = (1 - D_1 - D_2)T_s$$

Where, $T_s = t_1 + t_2 + t_3$

Whether energy sources are being gathered simultaneously or discretely will have an impact on the sort of switching mechanism that is used.

Steady State Analysis of Designed Triple Input Converter

This section develops and discusses the general methodology for analyzing any multi input converter (MIC). Power electronic switches, an inductor, and capacitors make up the converter. The developed method is entirely based on the methodology and arguments used for analyzing single-input converters. Prior to analyzing the MIC, the volt-second and ampere-second balance principles for capacitors and inductors are briefly discussed. In addition, that small signal approximation has been taken into account throughout the analysis. These guidelines and approximations make it easier to derive the output voltage expression and analyze the MIC's inductor current and capacitor voltage. In order to keep things simple and avoid difficult calculations, the examination of the suggested MIC is conducted under the following presumptions: (i) The converter operates in a steady state, and continuous current flow is the mode of current conduction. (ii) The designed converter has been realized using lossless components i.e., inductor, capacitor and switches do not dissipate power (passive components are considered free from any loss due to switching and voltage drop due to absence of resistance), (iii) It is anticipated that the output capacitor will provide a steady output voltage.

Small Signal Approximation

It is quite challenging to create a suitable filter for a switch mode power converter that can pass low frequency signals while blocking switching frequency components and ripple associated with them. Because of this, the output voltage has some ripple content from switching operation. The output shown in Figure 4, can be mathematically presented as,

$$v_o(t) = V_o + v_{ripple}(t) \quad (1)$$

Where, $v_o(t)$ = actual voltage across load, which contains the desirable DC components V_o and small ripple content $v_{ripple}(t)$ generated from switching action.

Small signal-ripple or linear-ripple approximation is the most used approximation technique. It significantly simplifies the study of the various waveforms of the suggested TIC.

Principle of Volt-Second Balance pertaining to Inductor

The waveforms of the voltage across and current through the inductor for single input switch mode converters operating in equilibrium for a single switching cycle are illustrated in Fig. 4 in steady state conditions. According to the application of the inductor volt-second balance principle, the net change in current

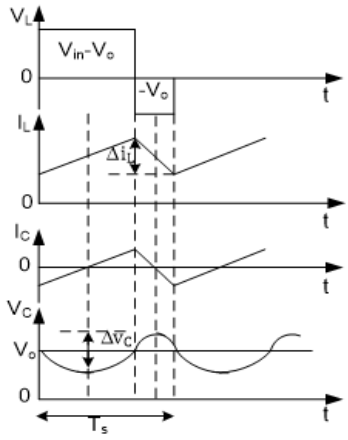

Figure 4. Voltage across Inductor, Current and output voltage of conventional Buck converter

flowing through the inductor under steady-state circumstances for one switching cycle should be zero. The voltage across the inductor can be expressed as,

$$v_L(t) = L\frac{di_L(t)}{dt} \quad (2)$$

For one complete switching cycle on integrating both the sides, we get

$$i_L(t) - i_L(0) = \frac{1}{L}\int_0^{T_s} v_L(t)\,dt \quad (3)$$

It is clear from the equation above that, for a single switching cycle, Throughout the same cycle, the integral of the applied inductor voltage equals or is proportional to the net change in inductor current. The start and end values of the current flowing through the inductor coincide at a steady state. This means that, as indicated in Equation 4, the integration of the voltage across the inductor under the time restriction of zero to steady state will be equal to zero.

$$\int_0^{T_s} v_L(t)\,dt = 0 \quad (4)$$

Therefore, the average inductor voltage

$$V_O = \int_0^{T_s} v_L(t)\,dt = 0 \quad (5)$$

In the equilibrium situation, the voltage that appears across the inductor has an assumed average value or DC component of zero.

Capacitor Ampere-Second Balance

Figure 4 shows the steady-state waveform of capacitor current and voltage for single input switch mode converters operating in equilibrium for a single switching cycle. The net change in voltage that appears across the capacitor over the course of a single switching cycle and in a steady state situation should be zero, according to the capacitor ampere-second balancing principle. The capacitor's current can then be measured via,

$$i_c(t) = C\frac{dv_c(t)}{dt} \quad (6)$$

By integrating of above equation for one switching cycle gives,

$$v_c(t) - v_c(0) = \frac{1}{C}\int_0^{T_s} i_c(t)\,dt \quad (7)$$

Figure 4 shows the steady state waveform of the capacitor current and voltage for single input switch mode converters that are running in equilibrium for a single switching cycle. According to the capacitor ampere-second balancing theory, the net change in voltage that appears across the capacitor over the course of a single switching cycle and in a steady state situation should be zero. After that, current via the capacitor can be measured using,

$$\int_0^{T_s} i_c(t)\,dt = 0 \quad (8)$$

Average value of current capacitor

$$i_{c\_ave} = \frac{1}{C}\int_0^{T_s} i_c(t)\,dt = 0 \quad (9)$$

This suggests that for equilibrium to exist, the average value or DC component of the current across the capacitor must equal zero.

TIC Mode of Operation

TIC Operation in Buck Mode

In order to determine the total amount of volt-seconds across the inductor during a single switching cycle, the following application of the inductor volt-second idea is used:

$U_{PV} = (V_{PV} - V_o);\ U_{BT} = (V_{BT} - V_o);\ U_{UC} = (V_{UC} - V_o)$

$U_1 = (V_{BT} + V_{UC});\ U_2 = (V_{PV} + V_{BT});\ U_3 = (V_{PV} + V_{BT} + V_{UC})$

$U_{BU} = (U_1 - V_o);\ U_{PB} = (U_2 - V_o);\ U_{PBU} = (U_3 - V_o)$

$\int_0^{T_s} v_L(t)\,dt = U_{PV}t_1 + U_{UC}t_2 + U_{BT}t_3 + U_{BU}t_4 + U_{PB}t_5 + U_{PBU}t_6 + (-V_o)t_7$

$V_{PV}(t_1 + t_4 + t_6) + V_{BT}(t_2 + t_5 + t_6) + V_{UC}(t_3 + t_5 + t_6) - V_o(T_s) = 0$

$V_{PV}(t_1 + t_4 + t_6) + V_{BT}(t_2 + t_5 + t_6) + V_{UC}(t_3 + t_5 + t_6) = V_o(T_s)$

$$V_{PV}D_{PV} + V_{BT}D_{BT} + V_{UC}D_{UC} = V_o \quad (10)$$

Where,

$$T_s = t_1 + t_2 + t_3 + t_4 + t_5 + t_6 + t_7;\ \ t_7 = t_{OFF}$$

Duty cycle of PV, $D_{PV} = \frac{\text{PV on time}(t_1+t_5+t_6)}{T_s}$;

Duty cycle of BT, $D_{BT} = \frac{\text{BT on time}(t_3+t_4+t_5+t_6)}{T_s}$;

Duty cycle of UC, $D_{UC} = \frac{\text{UC on time}(t_2+t_4+t_6)}{T_s}$

From Equation 9, it can be concluded that, for lossless system,

$P_{Input} = P_{Output}$

$$V_{PV}I_{PV} + V_{BT}I_{BT} + V_{UC}I_{UC} = V_oI_o \quad (11)$$

Figure 5 depicts the various operational stages of a triple input converter working in Buck mode with separate switching pulses. In this mode, input voltages VPV, VBT, and VUC are applied across the inductor, respectively, at the t_1, t_2, t_3, t_4, t_5 *and* t_6 time periods. Negative voltage -V_O is seen across the inductor during time interval t_7. Table 1 provides a summary of the in-depth analysis of TIC operation in Buck mode.

The value of inductance and capacitance for the designed TIC operation in Buck mode can be calculated as;

$$L = \frac{V_o}{\Delta i_L f_s}\left(1 - (D_{PV} + D_{BT} + D_{UC})\right) \quad (12)$$

$$C = \frac{V_o}{8L\Delta v_c f_s^2}\{1 - (D_{PV} + D_{BT} + D_{UC})\} \quad (13)$$

Table 1. Different Working Stages in Buck Mode of Operation (V1 > V2)

State	Conducting Switches	Active Source	Inductor Voltage	Inductor Status
1	S_1, S_3, D_2	V_{PV}	V_{PV}-V_O	Charging
2	S_2, S_3, D_2	V_{BT}	V_{BT}-V_O	Charging
3	S_2, S_4, D_2	V_{UC}	V_{UC}-V_O	Charging
4	SS_1, S_3, D_2	V_{PV}+V_{BT}	V_{PV}+V_{BT} -V_O	Charging
5	SS_2, S_2, D_2	V_{BT} +V_{UC}	V_{BT}+V_{UC}-V_O	Charging
6	SS_1, SS_2, D_2	V_{PV}+V_{BT} +V_{UC}	V_{PV}+V_{BT}+V_{UC}-V_O	Charging
7	D_1, D_2	Free wheeling	-V_O	Discharging

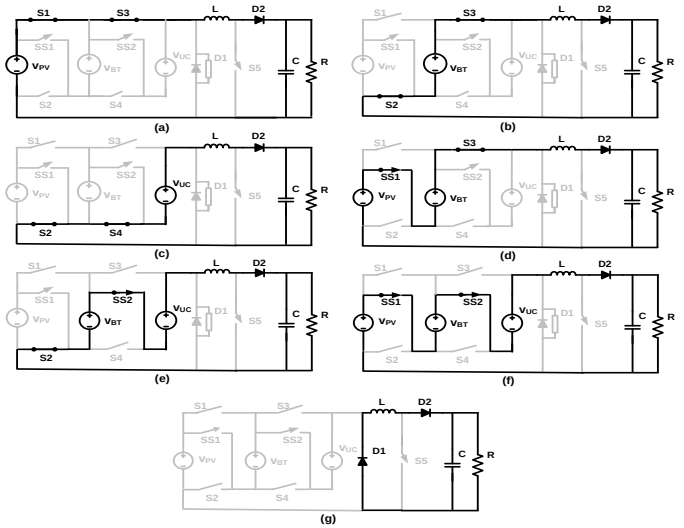

Figure 5. Different working states of the designed TIC in Buck mode of operation

TIC Operation in Boost Mode

The different states of TIC operation in Boost mode and for independent switching pulses are shown in Figure 6.

For time intervals t_1 *to* t_7, input voltages are provided across the inductor for TIC operation in the boost mode, accordingly. Negative voltage U3- V_O is seen across the inductor during time interval t_7. Table 2 provides a summary of the comprehensive investigation of TIC operation in Boost mode. By displaying several theoretical waveforms related to the converter, it is possible to analyze the operation of the Boost converter in greater depth. It is determined by using the volt-second balance concept to construct a relationship between the converter's input and output voltage that;

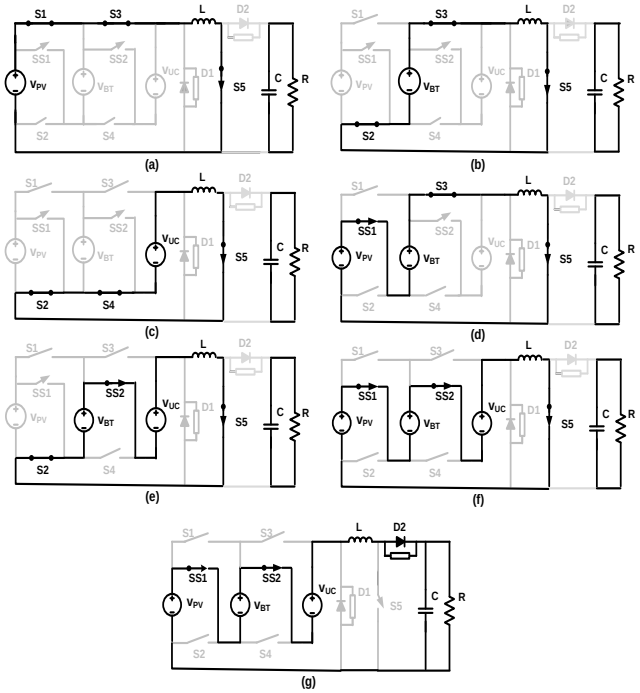

Figure 6. Different working states in Boost mode of operation

$$V_o = \frac{V_{PV}D_{PV}+V_{BT}D_{BT}+V_{UC}D_{UC}}{(1-D_{PV}-D_{BT}-D_{UC})} \quad (17)$$

Similarly, the input-output current relation can be obtained as;

$$I_o = \frac{(V_{PV}I_{PV}+V_{BT}I_{BT}+V_{UC}I_{UC})(1-D_{PV}-D_{BT}-D_{UC})}{V_{PV}D_{PV}+V_{BT}D_{BT}+V_{UC}D_{UC}}$$

These formulas can be used to determine the inductance and capacitor values:

$$L = \frac{V_o}{\Delta i_L f_s}(1-(D_{PV}+D_{BT}+D_{UC})) \quad (18)$$

$$C = \frac{V_o}{R\Delta v_c f_s} \times (t_{PV}+t_{BT}+t_{UC}) \quad (19)$$

Table 2. Different Working States of TIC in Boost Mode (V2 > V1)

State	Conducting Switches	Active Source	Inductor Voltage	Inductor Status
1	S_1, S_3, S_5	V_{PV}	V_{PV}-0	Charging
2	S_2, S_3, S_5	V_{BT}	V_{BT}-0	Charging
3	S_2, S_4, S_5	V_{UC}	V_{UC}-0	Charging
4	SS_1, S_3, S_5	V_{PV}+V_{BT}	V_{PV}+V_{BT} -0	Charging
5	SS_2, S_2, S_5	V_{BT} +V_{UC}	V_{BT}+V_{UC}-0	Charging
6	SS_1, SS_2, S_5	V_{PV}+V_{BT}+V_{UC}	V_{PV}+V_{BT}+V_{UC} -0	Charging
7	SS_1, SS_2, D_2	V_{PV}+V_{BT}+V_{UC}	V_{PV}+V_{BT}+V_{UC} -V_O	Discharging

Simulation And Result

The designed triple input converter's topology is simulated by the MATLAB/Simulink environment to assess its performance. Figure 7 depicts this structure. The modelling work makes use of three different input sources: a solar photovoltaic source, a battery storage system, and an ultra-capacitor bank. The converter is constantly operated in the buck, boost, and buck-boost modes before the entire collection of data is reviewed under steady state settings.

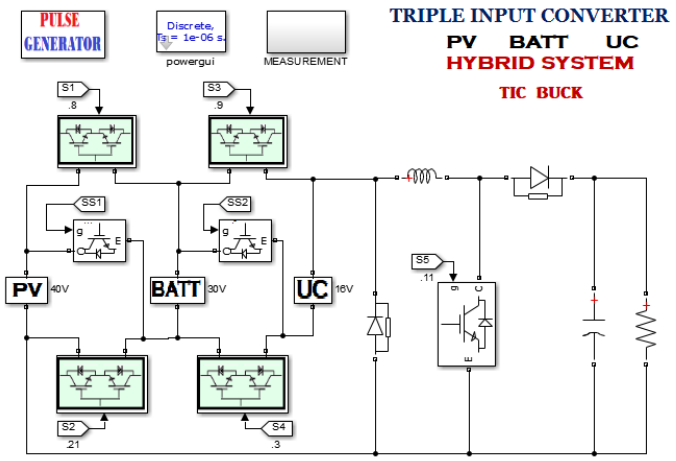

Figure 7. Simulation model of the designed TIC

Results of designed TIC's Simulation in Buck Mode

Figures 8 and 9 illustrate the voltage across the inductor, current through the inductor, voltage across the load, and current through the load, respectively, for converter operating in buck mode.

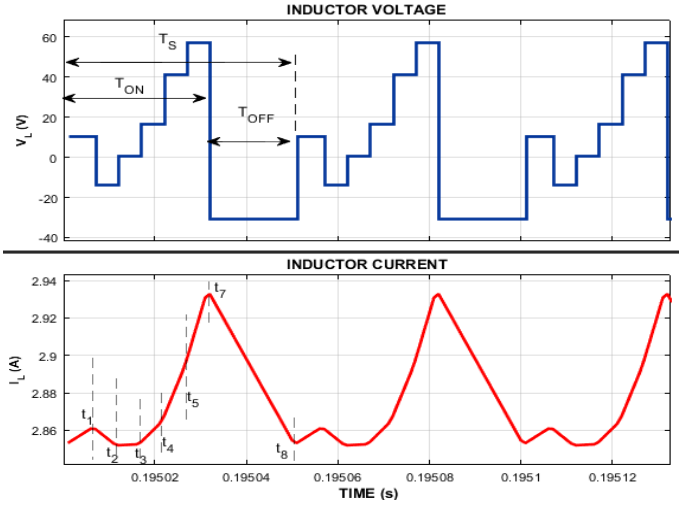

Figure 8. Voltage across inductor and current through inductor for converter operation in Buck mode

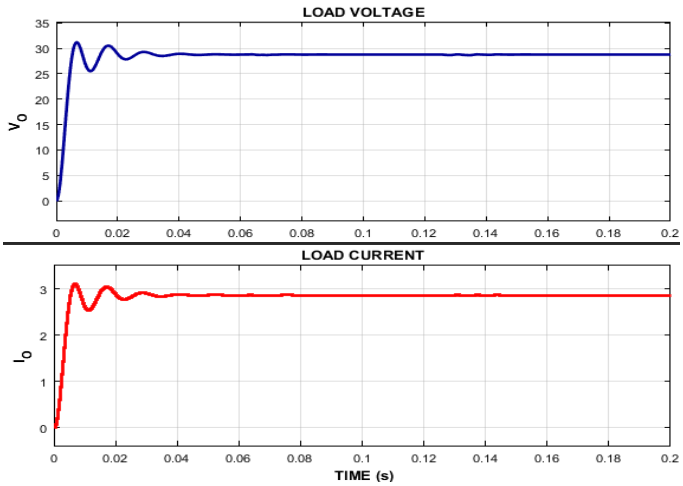

Figure 9. Current flow through the load and voltage across the load during converter operating in Buck mode

Simulation Results of Designed TIC in Boost Mode

Figures 10 and 11 show, respectively, the voltage across the inductor, the current through the inductor, and the voltage across the load for converter operation in boost mode.

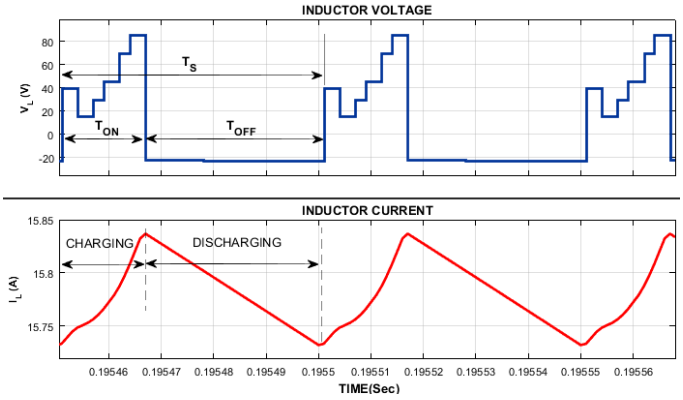

Figure 10. Voltage across Inductor and current through inductor for converter operation in boost mode

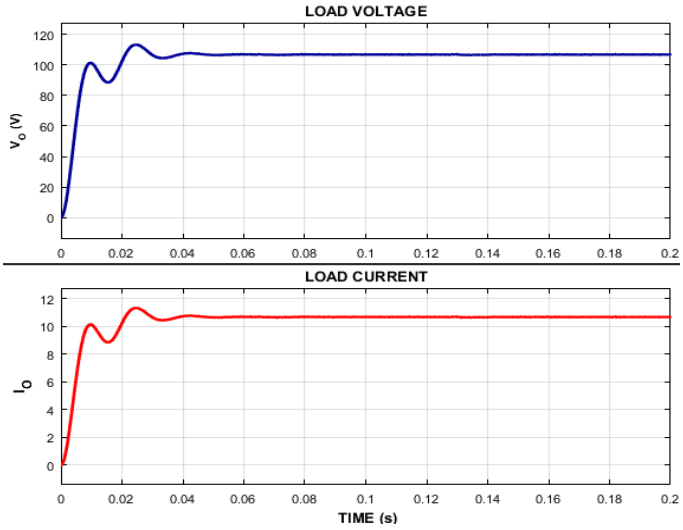

Figure 11. Current flow through the load and voltage across the load for converter operating in boost mode

Discussion

The topologies described in the study can combine several energy sources of various ratings. Three separate energy sources (PV, battery, and UC), each with a different voltage current characteristic, can be harvested using the suggested topologies. It functions well as a buck converter and boost converter and offers the option of connecting the load alone or in bulk in series (or parallel), depending on the load's needs.

According to the outcomes of the simulation work, the suggested converters are capable of not only obtaining energy from various sources with various properties (in the present case, PV, Battery, and UC), but they also provide a higher level of source electability, flexibility, and availability. Other features of the converter include simplifying the integration of renewable energy sources and enhancing the hybrid energy system's capacity for power sharing. The suggested converter's benefits include its ability to save time, lower component count, and control approach that does not involve complicated mathematical procedures.

Future Applicability

Future power generation industry projections indicate that renewable energy sources will dominate. Power electronics interface needs to be effective and dependable. In the study mentioned above, a number of power electronics converters were presented to address various problems such as high multiinput-multioutput interface, high efficiency, reliability, low cost, minimum number of components, and less power loss on an individual basis. However, no single circuitry is available that can address these problems on an overall basis. To create a circuitry that can effectively match supplies and loads that are changing instantly, more study must be done.

Conclusion

The designed topologies in this study can be used to harvest three different energy sources: PV, battery, and UC, with a range of voltage current (VI) characteristics. The recommended TIC, which is an expansion of the Double Input Converter (DIC), can link the load singly or in a group in series (or parallel), depending on the needs of the load. The offered TIC topologies function well because of thorough modeling and mathematical study of converters operating as buck converters, boost converters, and buck-boost converters. Based on the results of the simulation work, we were able to draw the conclusion that the suggested converters can obtain energy from a variety of sources with a variety of characteristics (PV, Battery, and UC), as well as offering a higher degree of source electability, flexibility, and availability. The converter's additional features also facilitate the use of renewable energy sources and improve the power-sharing capabilities of hybrid energy systems (HESS).

References

1. L. Kumar, S. Jain. Multiple-input DC/DC converter topology for hybrid energy system. *IET Power Electron.* **2013**, 6 (8), 1483–1501.
2. N.K. Reddi, M.R. Ramteke, H.M. Suryawanshi, K. Kothapalli, S.P. Gawande. An Isolated Multi-Input ZCS DC-DC Front-End-Converter Based Multilevel Inverter for the Integration of Renewable Energy Sources. *IEEE Trans. Ind. Appl.* **2018**, 54 (1), 494–504.

3. S. Khosrogorji, M. Ahmadian, H. Torkaman, S. Soori. Multi-input DC/DC converters in connection with distributed generation units – A review. *Renew. Sustain. Energy Rev.* **2016**, 66, 360–379.
4. Y. Li, X. Ruan, D. Yang, F. Liu, C.K. Tse. Synthesis of multiple-input DC/DC converters. *IEEE Trans. Power Electron.* **2010**, 25 (9), 2372–2385.
5. A.H. Chander, L.K. Sahu, S. Ghosh, K.K. Gupta. Comparative analysis on selection and synthesis of multiple input converters: A review. *IET Power Electron.* **2020**, 13 (4), 611–626.
6. C. Nagesha, N.K. Reddi, N. Lakshminarasamma. Multi input bidirectional resonant converter for hybrid energy systems. *9th IEEE Int. Conf. Power Electron. Drives Energy Syst. PEDES 2020* **2020**, 4–9.
7. S. Athikkal, G.G. Kumar, K. Sundaramoorthy, A. Sankar. Performance Analysis of Novel Bridge Type Dual Input DC-DC Converters. *IEEE Access* **2017**, 5 (c), 15340–15353.
8. C. Gupta, V.K. Aharwal. Optimizing the performance of Triple Input DC-DC converter in an Integrated System. *J. Integr. Sci. Technol.* **2022**, 10 (3), 215–220.
9. R. Jain, A. Laddha, N. Satyanarayana. DC-DC converter and its multiport interface. *2019 IEEE 16th India Counc. Int. Conf. INDICON 2019 - Symp. Proc.* **2019**, 1–4.
10. S.A. Gorji, H.G. Sahebi, M. Ektesabi, A.B. Rad. Topologies and control schemes of bidirectional DC–DC power converters: An overview. *IEEE Access* **2019**, 7, 117997–118019.
11. D. Navamani. Multi-Input DC-DC Converter Topologies-A Review. **2016**, 2230–2233.
12. A. Rajulapati, M. Prabhakar. INTERNATIONAL JOURNAL of RENEWABLE ENERGY RESEARCH Comparison of Non-isolated High Gain Multi-input DC-DC Converters. **2021**, 11 (3).
13. J. Huang, Y. Wang, Z. Li, W. Lei. Unified Triple-Phase-Shift Control to Minimize Current Stress and Achieve Full Soft-Switching of Isolated Bidirectional DC-DC Converter. *IEEE Trans. Ind. Electron.* **2016**, 63 (7), 4169–4179.
14. A. Affam, Y.M. Buswig, A.K.B.H. Othman, N. Bin Julai, O. Qays. A review of multiple input DC-DC converter topologies linked with hybrid electric vehicles and renewable energy systems. *Renew. Sustain. Energy Rev.* **2021**, 135 (August 2020), 110186.
15. T.K. Santhosh, C. Govindaraju. Dual input dual output power converter with one-step-ahead control for hybrid electric vehicle applications. *IET Electr. Syst. Transp.* **2017**, 7 (3), 190–200.
16. L.W. Zhou, B.X. Zhu, Q.M. Luo. High step-up converter with capacity of multiple input. *IET Power Electron.* **2012**, 5 (5), 524–531.
17. R.R. Ahrabi, H. Ardi, M. Elmi, A. Ajami. A Novel Step-Up Multiinput DC-DC Converter for Hybrid Electric Vehicles Application. *IEEE Trans. Power Electron.* **2017**, 32 (5), 3549–3561.
18. E. Amiri, R.R. Khorasani, E. Adib, A. Khoshkbar-Sadigh. Multi-Input High Step-Up DC-DC Converter with Independent Control of Voltage and Power for Hybrid Renewable Energy Systems. *IEEE Trans. Ind. Electron.* **2021**, 68 (12), 12079–12087.
19. A. Kumar, Smrity, N. Bajoria, A. Alam. Modeling and Analysis of Multi-Input Hybrid DC-DC Converter in an Integrated System. *Proc. - Int. Conf. Vis. Towar. Emerg. Trends Commun. Networking, ViTECoN 2019* **2019**, 1–6.
20. F. Nejabatkhah, S. Danyali, S.H. Hosseini, M. Sabahi, S.M. Niapour. Modeling and control of a new three-input dc-dc boost converter for hybrid PV/FC/battery power system. *IEEE Trans. Power Electron.* **2012**, 27 (5), 2309–2324.